Tikrit Journal of Pure Science Vol. 31 (3) 2026

DOI: *https://doi.org/10.25130/tjps.v31i3.2003*

IRAQI Academic Scientific Journals

Tikrit Journal of Pure Science

ISSN: 1813 – 1662 (Print) --- E-ISSN: 2415 – 1726 (Online)

Journal Homepage: https://tjpsj.org/

Tikrit Journal of Pure Science

Petrophysical Characteristic of the Lower Jurassic Formations in the Miran Oil Field, Kurdistan region/ NE Iraq

Shewa N. Karim[1], Fouad M. Qader[2]

[1,2]Department of Earth Sciences and Petroleum, College of Science, University of Sulaimani, Kurdistan Region, Iraq

Received: 20 Apr. 2025 **Received in revised forum:** 26 Mayr. 2025 **Accepted:** 11 Jun. 2025

Final Proofreading: 28 Jun. 2025 **Available online:** 25 Jun. 2026

ABSTRACT

This study focuses on evaluating the Lower Jurassic Formations within the Miran Oil Field, located in Northeastern Iraq. A detailed analysis was conducted using well log data from the Alan, Mus, and Adaiyah formations encountered in the Miran-2 (MW-2) Well, with supplementary stratigraphic and lithological information from wells ME-1 and MW-3. The investigation employed both quantitative and qualitative well-log data, including Gamma Ray, Sonic, Density, Neutron, and Photoelectric Factor logs, rate of penetration (ROP), and gas chromatographic profiles. Additional datasets, such as Logging While Drilling (LWD), Measurement While Drilling (MWD), well reports, and master logs, were also used.

The results indicate that the upper part of the Lower Jurassic interval, comprising the Alan and Mus formations, is predominantly composed of carbonate rocks interbedded with shale, with intermittent evaporite bands. The presence and thickness of evaporite rocks increase downward, eventually dominating the lower part of the section, represented by the Adaiyah formation.

Due to the prevalence of shale in the upper units and evaporites in the lower units, the studied section lacks favorable reservoir characteristics. Porosity is generally classified as poor to negligible, and permeability is similarly low. Based on threshold values of 35% shale content, 0.1 millidarcy permeability, and 0.07 porosity, it was determined that of the 148-meter total thickness of the Alan, Mus, and Adaiyah formations, 26 meters are shale-dominated and 67.5 meters are evaporite-rich. Of the remaining 54.5 meters of carbonate lithology, only a total of 2.5 meters exhibit porosity and permeability values that exceed the minimum thresholds required for effective reservoir rocks.

Consequently, the study concludes that the Lower Jurassic successions in the Miran Oil Field do not constitute a viable hydrocarbon reservoir. However, due to its lithological composition, particularly the extensive evaporite and shale layers, it may serve as an effective seal rock for underlying reservoirs, such as the Butmah and Kurra Chine formations.

Keywords: Adaiyah formation, Alan formation, Lower Jurassic formations, Miran oil field, Mus formation, Well log analysis.

Name: Shewa N. Karim **E-mail:** shewa.karim@univsul.edu.iq

Tikrit Journal of Pure Science Vol. 31 (3) 2026
DOI: *https://doi.org/10.25130/tjps.v31i3.2003*

الخصائص البتروفيزيائية لتكوينات الجوراسي السفلي في حقل ميران النفطي، إقليم كوردستان / شمال شرق العراق

شيوه نوزاد كريم[1]، فؤاد محمد قادر[2]

[2,1]قسم علوم الأرض والنفط، كلية العلوم، جامعة السليمانية، إقليم كوردستان، العراق

الملخص

تركز هذه الدراسة على تقييم تكوينات العصر الجوراسي السفلي في حقل ميران النفطي، الواقع شمال شرق العراق. أُجري تحليل مُفصّل باستخدام قرآت سجلات الآبار من تكوينات علان، موس، وعداية المخترقة في بئر ميران-2 **(MW-2)**، بالإضافة إلى معلومات طباقية وصخارية مُكمّلة مُستمدة من البئرين **ME-1** و**MW-3**. استخدم البحث بيانات سجلات الآبار بشكل كمي و نوعي، في مجسات أشعة غاما، الكثافة، الصوتية، النيوترون، والعامل الكهروضوئي، بالإضافة إلى سجلات الكاليبر، ومعدل الاختراق **(ROP)**، وكروماتوغرافيا الغاز. كما استُخدمت مجموعات بيانات إضافية مثل تسجيل الآبار أثناء الحفر **(LWD)**، والقياس أثناء الحفر **(MWD)**، وتقارير الآبار، والسجلات الرئيسية. تشير النتائج إلى أن الجزء العلوي من ترسبلت فترة الجوراسي السفلي التي تضم تكويني علان وموس يتكون في الغالب من صخور كربوناتية متداخلة مع طبقات الصخر الطيني، إلى جانب نطاقات متقطعة من صخور متبخرة. يزداد وجود وسمك صخور المتبخرة نزولًا، ليهيمن في النهاية على الجزء السفلي من المقطع، الذي يمثله تكوين عداية. ونظرًا لانتشار الصخر الطيني في الوحدات العليا والمتبخرات في الوحدات السفلية، فإن المقطع المدروس يفتقر إلى الخصائص المكمنية. تُصنف المسامية عمومًا على أنها ضعيفة إلى مهملة، والنفاذية منخفضة ايضا. واستنادًا إلى قيم عتبة محتوى االطين بنسبة 35٪، ونفاذية 0.1 مليدارسي، ومسامية 0.07، فقد تم تحديد أنه من إجمالي سمك تكوينات علان، موس، وعداية البالغ 148 مترًا، يهيمن الصخر الطيني (محتوى الطين) على 21.5 مترًا و المتبخرات 64.5 مترًا. من بين الـ 62 مترًا المتبقية من الصخور الجيرية، لا يبقى سوى 2.5 متر حيث قيم المسامية والنفاذية تتجاوز الحد الأدنى المطلوب لصخور المكمن الفعالة. ونتيجةً لذلك، خلصت الدراسة إلى أن تتابعات العصر الجوراسي السفلي في حقل ميران النفطي لا تُشكل مكمنًا هيدروكربونيًا قابلًا للاهتمام. ومع ذلك، نظرًا لتركيبها الصخري، وخاصةً طبقات المتبخرات والصخر الطينية الواسعة، مما يجعلها غطاءً جيدًا للوحدات المكمنية المحتملة الواقعة تحتها، مثل تكوين بطمة.

INTRODUCTION

The Jurassic succession plays a crucial role in the petroleum systems of the Arabian Plate, significantly contributing to hydrocarbon generation, migration, and entrapment. During the Jurassic Period, the Arabian Plate lay within the equatorial zone and experienced relative tectonic stability, resulting in the deposition of organic-rich sediments. These deposits, comprising a sequence of shallow marine carbonates and siliciclastic facies, exhibit high porosity and permeability, making them excellent reservoir units. Subsequent deposition of impermeable evaporites or other non-permeable sediments created effective seal formations, leading to the development of closed petroleum systems. As a result, Jurassic and Cretaceous sequences across Saudi Arabia, Iraq, and the broader Arabian Gulf region have emerged as some of the most prolific hydrocarbon-bearing units[(1-5)].

In Iraq, the Jurassic succession is of particular significance, as it consists of organic-rich source rocks, carbonate reservoirs with favorable petrophysical properties, and evaporitic seals that collectively enhance hydrocarbon potential. In recent years, numerous studies conducted by Iraqi geologists [(6-24)] highlighted the significant role of

formation sequences, which are most prominent in the northern and northeastern regions, particularly within the Zagros Fold-Thrust Belt and the Mesopotamian Foreland Basin. The region underwent extensive marine transgressions during the Early Jurassic (Toarcian) period, resulting in the deposition of a variety of facies, from non-deposition and erosion in Southern Iraq to clastic-dominated platforms in the West and shallow marine carbonate platforms in the North and East. [25, 26]. Within this stratigraphic framework, the Lower Jurassic Alan, Mus, and Adaiyah formations were deposited in restricted marine to lagoonal environments under fluctuating sea levels and tectonic subsidence. [25, 27].

The Alan Formation, primarily composed of anhydrite and dolomitic limestones, formed in a restricted lagoonal to evaporitic environment and serves as an effective seal, preventing hydrocarbon migration. [28]. The Mus Formation, characterized by bioclastic limestone and dolostone, serves as a significant reservoir due to its high porosity and permeability.[5,29]. Meanwhile, the Adaiyah formation, consisting of interbedded shales, carbonates, and evaporites, serves a dual function as a potential source rock and an additional sealing unit.[25]. These Formations are laterally equivalent to the Sehkaniyan Formation in Northeastern Iraq, with distinct facies variations corresponding to different depositional environments. [25].

The present study focuses on the petrophysical characterization of the Alan, Mus, and Adaiyah formations in the Miran Oil Field, Kurdistan Region, Northeastern Iraq. The research is based on well log data from MW-2, with supplementary information from MW-3 and ME-1 wells. The study aims to (1) analyze the lithology and mineralogical composition of these formations, (2) evaluate their reservoir properties, and (3) assess thickness variations and identify productive hydrocarbon-bearing zones. These insights are critical for improving the understanding of the Jurassic petroleum system in the region and optimizing hydrocarbon exploration strategies.

GEOLOGICAL SETTING

The Miran Field, located in Northeastern Iraq, is a significant natural gas or condensate reserve discovered in 2011 by Heritage Oil Company. The Miran Block lies within Iraq's High-Folded Zone and is situated between the Surdash and Piramagrun anticlines to the northeast. The Khaldan syncline, along with the Darbandi Bazian-Hanjira-Sagrma-Qaradagh anticline (as presented in Fig.1), includes several wells, MW-2, MW-3, and ME-1, that have significantly contributed to the geological understanding and formation evaluations of the area. The first study, MW-2, was spudded in November 2009 and reached a total depth of approximately 4426m, terminating in the Galikhana Formation. It encountered a drilled thickness of approximately 670m, with the Lower Jurassic succession extending between 2480m and 3150m measured depth. [30, 31]. Additionally, MW-2 helped define the field's structural and stratigraphic characteristics within a total area of 1015 km². The second well, MW-3, served as an appraisal well targeting the Cretaceous and Jurassic formations. It was drilled as a sidetrack to extend the depth of MW-1, which had failed to reach its planned target due to drilling complications. MW-3 was spudded in August 2011 and ultimately reached a total depth of 3528m, further enhancing the reservoir evaluation and hydrocarbon potential of the Miran Field.

Structural Framework

The Miran anticlinorium extends approximately 70 km in length and 15 km in width, exhibiting a northwest-southeast orientation consistent with the broader structural trend of the Zagros Fold-Thrust Belt. The anticlinorium comprises two primary anticlines, Miran East and Miran West, which are separated by significant NW–SE-oriented thrust faults (as presented in Fig. 2). Notably. The Miran West anticline exhibits a steeper southwestern limb compared to other folds within the High-Folded Zone.

DOI: *https://doi.org/10.25130/tjps.v31i3.2003*

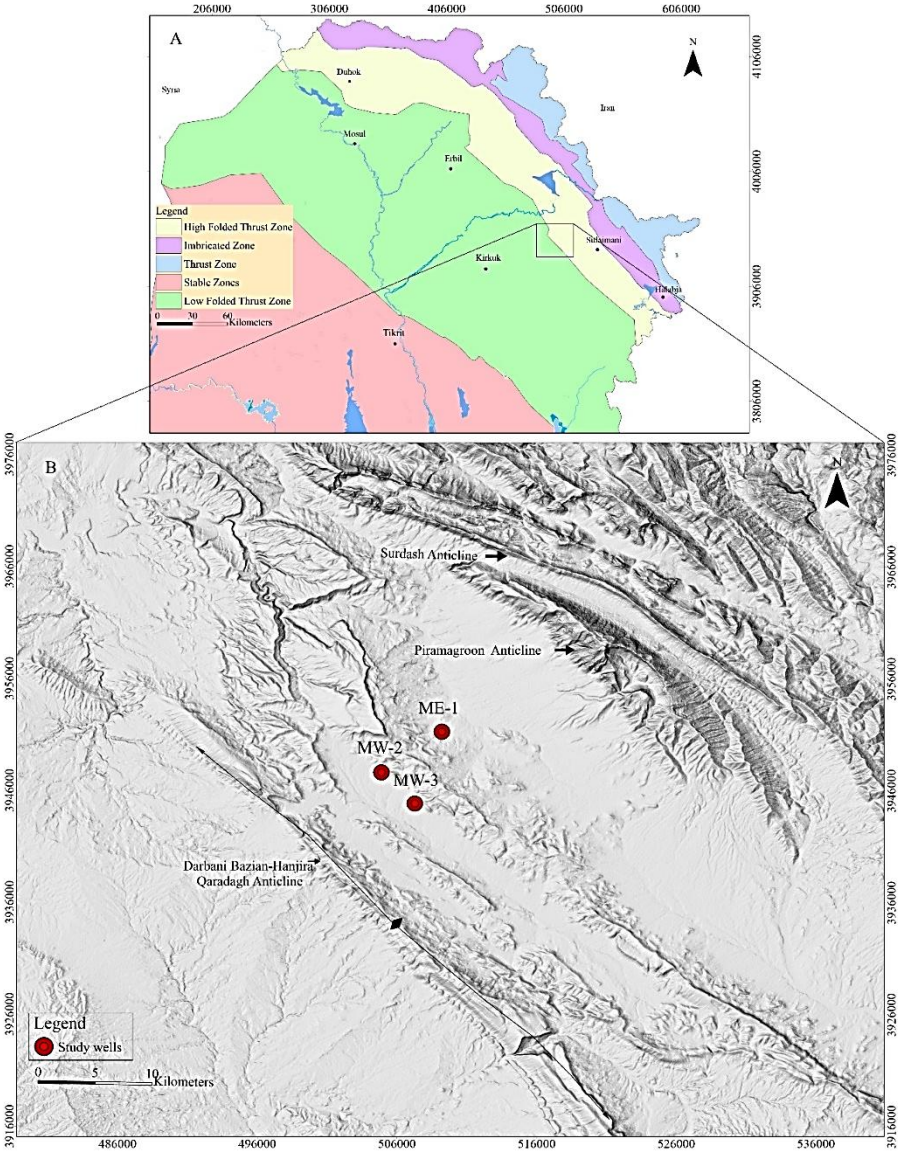

Fig. 1: Location map. A. Tectonic subdivision of Iraq depends on[25], B: Location of studied wells.

Miran East and Miran West are interpreted as uplifted fault-propagation folds associated with multiple hinterland-divergent listric faults.[32]. The structural complexity of Miran West is further accentuated by extensive thrusting within its core, which has contributed to significant deformation. [30].

DOI: *https://doi.org/10.25130/tjps.v31i3.2003*

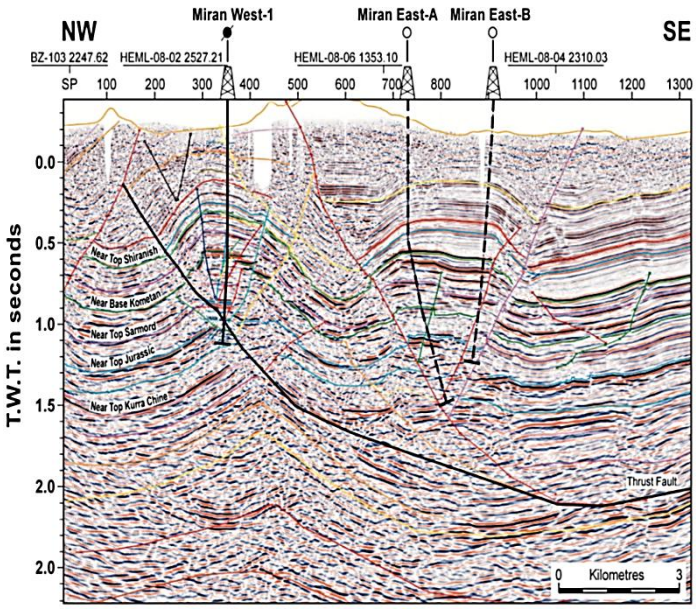

Fig. 2: The seismic section illustrates the subsurface structure of the Miran Field, extending from the Northwest (NW) to the Southeast (SE) along the dip [(33)]

Stratigraphy

The Lower Jurassic succession comprises the Ubaid, Hussainyat, and Amij formations of West Iraq's clastic-carbonate inner shelf. Wells in Central, Northern, and Eastern Iraq provide distinct definitions of the inner-shelf carbonate-evaporite formations of Butmah, Adaiyah, Mus, and Alan. The northern and northeastern High Folded Zone, with the Balambo-Tanjero Subzone, contains isolated lagoonal facies of the Sarki and Sehkaniyan formations.[(33-40)]In a lagoonal evaporite environment, the Liassic succession was deposited in a sabkha saline setting, except for the Imbricated Zone and the Northeast of the High-Folded Thrust Zone, where evaporite is subordinate. [(41)].

In the Miran Field, multiple wells have successfully encountered a well-preserved stratigraphic succession of Jurassic-age formations extending more than 800 m. This succession extends from the Chia Gara Formation at the top to the Butmah Formation at the base, encompassing the intervening Barsarin/Gotnia, Naokelekan, Sargelu (as illustrated in Fig. 3), Alan, Mus, and Adaiyah formations. The present study focuses specifically on the Alan, Mus, and Adaiyah formations.

DOI: *https://doi.org/10.25130/tjps.v31i3.2003*

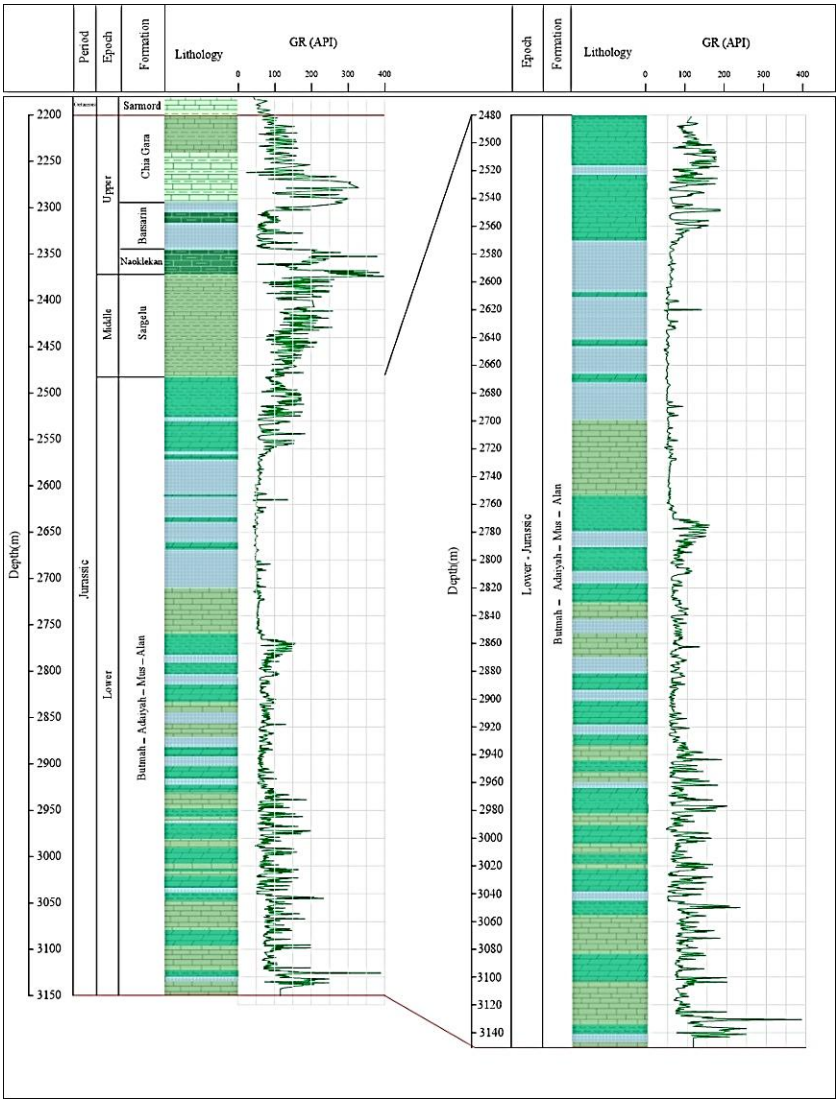

Fig. 3: Stratigraphic column of the Jurassic succession; the left panel displays the stratigraphic column and gamma-ray response of the Jurassic succession, including the Chia Gara, Barsarin, Naokelekan, Sargelu, Alan, Mus, Adaiyah, and Butmah formations within MW-2 well. In contrast, the right panel shows stratigraphic successions and gamma-ray responses of the Lower Jurassic succession in the MW-2 well, including the Alan, Mus, Adaiyah, and Butmah formations.

Alan Formation

Dunnington initially observed the Alan Formation in 1953 in the borehole Alan-1, northwest of Iraq, North of Mosul. It is characterized as an 87-meter-long intercalation of anhydrite and a subordinate carbonate layer. The conformable formations at the top and bottom were deposited in a basin-centered sabkha environment [25]. In certain locations, such as the Ain Zalah area, evaporitic lagoons are substituted by calcareous lagoonal or neritic environments [41]. The lithology of the formation primarily consists of bedded anhydrite with subordinate pseudo-oolitic limestone[25]. The formation gets replaced by the upper Sehkaniyan Formation in the north and northeast of the High Folded Zone, an Imbricated Thrust Zone. Given its stratigraphic position between the Middle Jurassic Sargelu Formation and the Liassic Mus Formation, a Liassic age is inferred [41]. According to the final report and mud log formats prepared by Heritage Oil Company [31], the estimated drilled thickness of the Alan Formation in well MW-2 is approximately 64 meters. This thickness exhibits a significant increase toward the southeast, reaching

178.4 meters in well MW-3 [42], and northeast 177.5m in well ME-1 [43] (as illustrated in Fig. 4).

Mus Formation

This formation was first identified by Dunnington in 1953 in the Butmah-2 Well, located in Northwest Iraq within a Low-Folded Thrust Zone. It is characterized by approximately 50 meters of argillaceous limestone that has undergone dolomitization, including poloidal limestone, with occasional interbeds of anhydrite and shale. Normal marine salinity conditions characterized the depositional environment of the Mus Formation. Its upper and lower boundaries are gradational and conformable with the overlying Alan Formation and the underlying Adaiyah Formation, respectively. [41]. The Mus Formation has surface equivalents in western Iraq, represented by the Amij Formation, and in the Kurdistan Region, where it corresponds to the middle section of the Sehkaniyan Formation. Chronostratigraphically, the Mus Formation is assigned to the Late Liassic, likely the Early Toarcian stage, with Lithiotis fossils indicating an age range from the Pliensbachian to Toarcian [25].

In the Miran field, the thickness of the Mus Formation varies significantly across wells, likely due to structural deformation and changes in depositional conditions. In MW-2, the formation attains a thickness of 28 meters, with the upper section composed primarily of compacted dolomitic limestone, shale, dolomite, and anhydrite, while the lower section transitions into dolomitic limestone interbedded with anhydrite.[31]. In contrast, ME-1 and MW-3 record substantially greater thicknesses of 74 and 109.4 meters, respectively [42, 43], (as shown in Fig.4).

Adaiyah Formation

The first indication of the Adaiyah Formation has been identified in the Adaiyah-1 Well, positioned north of the Foothill Zone (Low Folded Thrust Zone), west of Mosul. [44], containing 90 meters of shale, limestone, and nodular anhydrite [5]. The Adaiyah Formation is absent in Northwest Iraq, in well Khlesia-1, which is attributed to truncation beneath the Lower Senonian unconformity.

The formation exhibits gradational and conformable contacts at both its lower and upper boundaries; it is bordered above by the Mus Formation and below by the Butmah Formation. The depositional environment of this formation is a sabkha, dominated by lagoonal evaporite facies, located within an inner-shelf basin. [25, 44].

The age-equivalent units are identified as the upper section of the Hussainyat Formation in Western Iraq and the lower section of the Sehkaniyan Formation in the High-Folded, Imbricated Thrust Zone. [25]. The contact between the Adaiyah and Sehkaniyan formations is believed to be located along a buried structural uplift associated with the Dohuk-Chemchemal line (Ditmar and the Iraqi-Soviet Team, 1971, as referenced in [25].

Based on the final report and mud log data from Heritage Oil Company [31]The drilled thickness of the Adaiyah Formation in well MW-2 is estimated to be 56 meters. This thickness increases substantially, reaching 205.7 meters in well MW-3 and 132 meters in well ME-1.[42, 43], (as illustrated in Fig.4).

DOI: *https://doi.org/10.25130/tjps.v31i3.2003*

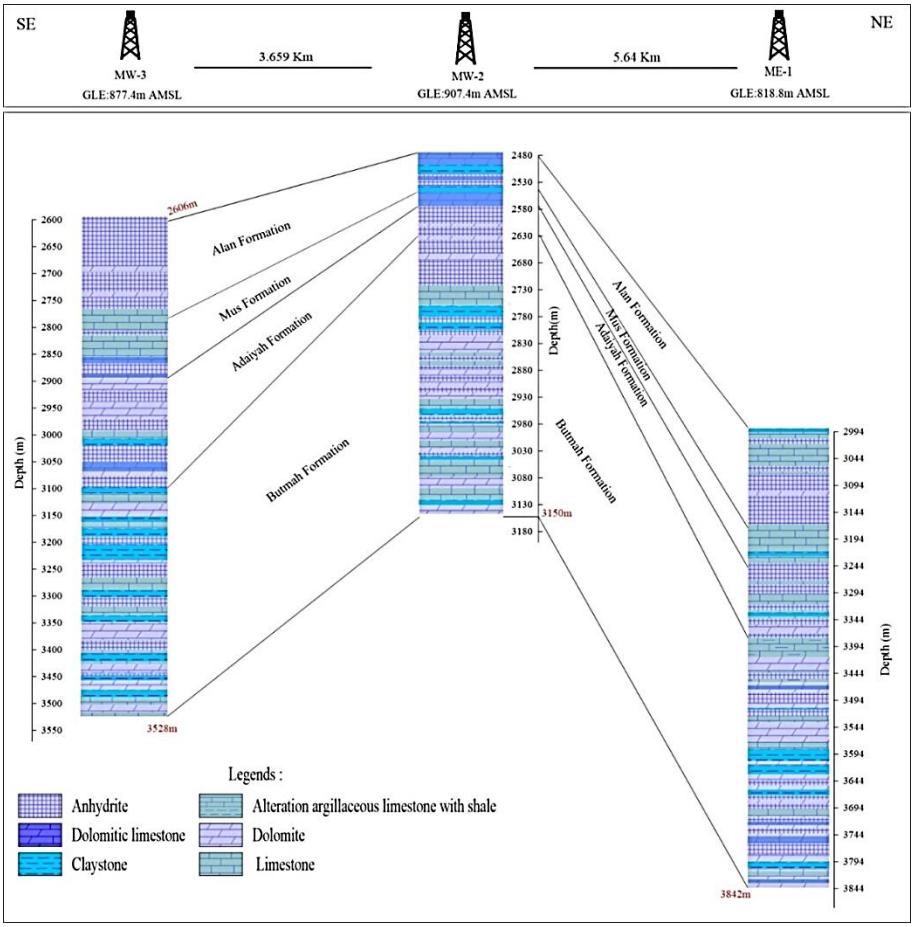

Fig. 4: Stratigraphic cross section from southeast to northeast that established MW-3, MW-2, and ME-1 wells, highlighting vertical and lateral lithological variations of the Butmah, Adaiyah, Mus, and Alan formations.

METHODOLOGY

The evaluation of these formations in the MW-2 was conducted using a suite of primary well-logging tools, including gamma-ray, sonic, density with photoelectric factor, neutron, and caliper logs. To enhance the accuracy and reliability of the data, Neural Log and Interactive Petrophysics software were used for digitization and environmental corrections. Furthermore, data acquired through measurement while drilling (MWD), including master logs, gas chromatograph, and final reports, were incorporated to calibrate and validate the results of the well-log analysis, ensuring a comprehensive and robust interpretation of the formation characteristics. Additionally, data from two additional wells, MW-3 and ME-1, were incorporated to provide a more comprehensive understanding of the study area.

RESULTS AND DISCUSSION

Lithology Identification

Petrophysical techniques are essential in subsurface exploration, providing data for lithological identification, particularly when core or sample material is unavailable. These methods play a significant role not only in reservoir characterization but also in lithological mapping [45,46]. emphasizes the importance of petrophysical analysis in such cases, especially when direct geological sampling is impractical. In this study, lithology was determined using key cross-plot techniques, including neutron porosity versus sonic transit time (NΦ-Δt), neutron porosity versus bulk density (NΦ-ρb), and photoelectric factor versus bulk density (PEF-ρb). Furthermore, data from Heritage Oil Company (31) were used as a reference to enhance lithological differentiation,

with the data calibrated against the obtained results.

Although the studied sections of the Lower Jurassic division in the Miran Field are subdivided into the Alan, Mus, and Adaiyah formations according to the final well reports, the presence of complex lithofacies, rapid rhythmic repetition, and gradational vertical changes, particularly in the upper part of the section, makes it difficult to distinguish formation boundaries clearly. Therefore, this study treats the entire interval as a single unit and uses the NΦ-Δt, NΦ-ρb, and PEF-ρb standard cross-plot techniques. When applying these cross-plots for lithological identification, the studied Jurassic interval shows a diverse range of rock types. For clarity and systematic classification, the lithologies have been categorized into three primary groups: dolostone (represented by a green cross), dolomitic limestone interbedded with shale (depicted by a pink star), and anhydrite (indicated by a blue rhombus). This classification framework facilitates a more structured interpretation of the subsurface geological characteristics.

NΦ- ρb cross-plot

Together with porosity values from the neutron logs, the density log serves as the fundamental lithology tool. Anhydrite and halite deposits may be distinguished from carbonate deposits by the density log, since they have different values between 1.9 and 3.0 g/cm3. Moreover, anhydrite can be distinguished from carbonate by the neutron log, which shows a negative value. In a carbonate sequence, limestone and dolostone are frequently distinguished with a combination of neutron and density log, as proposed by Schlumberger.[47], (as illustrated in Fig. 5).

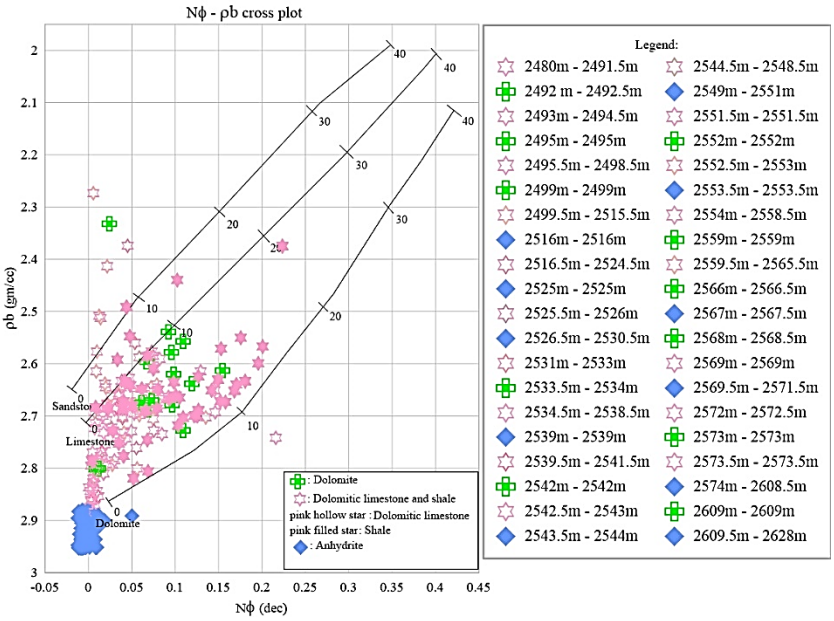

Fig. 5: Lithology identification from NΦ-ρb, cross plot for Adaiyah, Mus, and Alan formations in MW-2 Well [47].

(PEF-ρb) cross-plot

The photoelectric factor (PEF) curve, introduced with second-generation density tools (litho-tools), plays a key role in petrophysical analysis. It primarily reflects formation lithology, with minimal influence from porosity and pore fluids. The PEF, when combined with the density log, aids in lithology identification. [48].

The PEF–bulk density (ρb) cross-plot has been effectively used to determine lithology in Lower Jurassic formations from well MW-2. The cross-section reveals that the upper part is predominantly dolostone and dolomitic limestone, interbedded

with thin layers of shale and marl. In contrast, evaporite deposits become apparent at approximately 2516 meters in depth and repeat in a consistent pattern, eventually dominating the lower part of the section, as illustrated in the accompanying figure (Fig. 6).

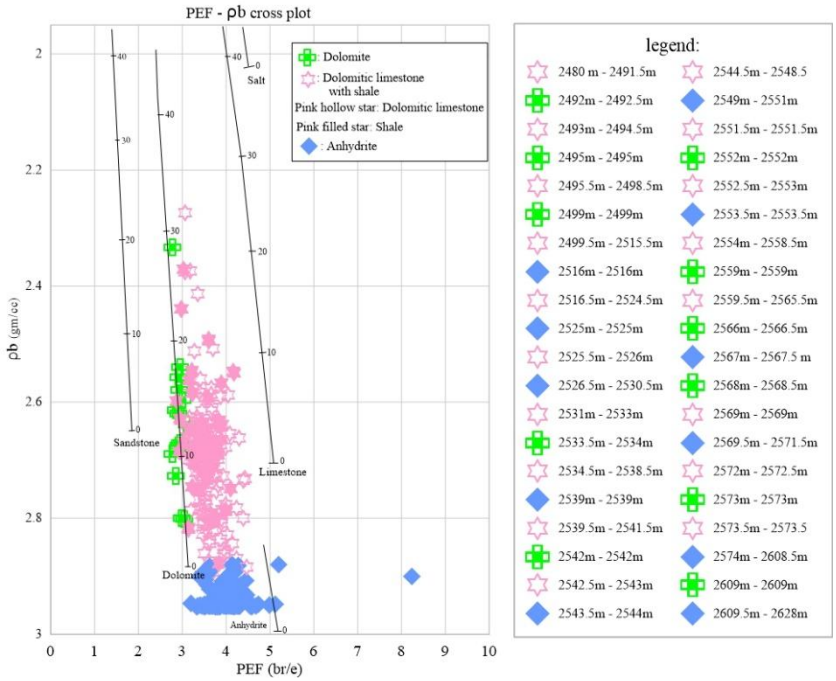

Fig.6: Lithology identification from PEF- ρb cross plot for Adaiyah, Mus and Alan formations in MW-2 [48] well.

NΦ- Δt cross-plot

The Neutron-Sonic (N-S) cross-plot uses well-log data from the neutron log and the acoustic wave travel-time log to identify different rock types. An N-S cross-plot can be used to differentiate between a single reservoir lithology and shale rock, as well as to detect evaporite minerals. [49]. In this regard, wireline well logs were used to understand the lithology types in the studied wells. The analyzed data in the wells MW-2 showed that the Lower Jurassic successions consist of repeating dolostone, dolomitic limestone, and evaporite (as illustrated in Fig.7)

Lithology between depths of 2480m and 2516 m includes dolomitic limestone intercalated with calcareous shale, with some thin layers of anhydrite between 2516 m and 2526 m. Calcareous shale was difficult to distinguish from the cross-plot due to its high calcareous content, which significantly increases its density compared to siliceous claystone. The average rate of penetration was approximately 1.51m/hr. [31].

DOI: https://doi.org/10.25130/tjps.v31i3.2003

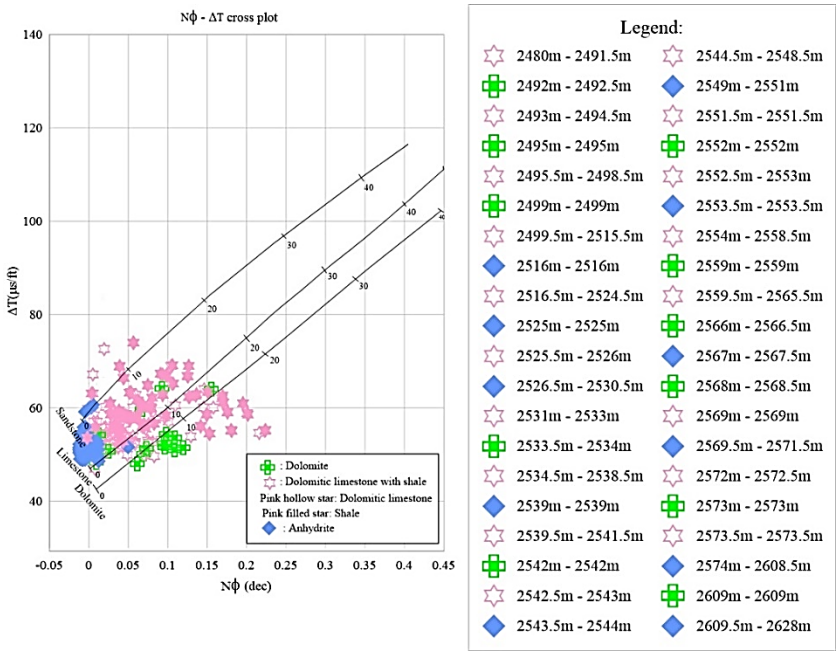

Fig.7: Representative lithology identification from NΦ- Δt, cross plot for Adaiyah, Mus and Alan formations in MW-2 well [49].

The interval between 2526.5-2530.5m was characterized by a thick layer (≈4m) of anhydrite that is observed by an elevated RHOB (ρb) value and a negative neutron porosity value (as presented in Fig.5). According to the mud log report, this interval covers most of the thickness of the Alan Formation, with an average rate of penetration of approximately 1.29m/hr. [31].

From 2531m to 2572m (lower part of Alan Formation and Mus Formation), the lithology comprises dolomitic limestone intercalated with calcareous shale, and thin evaporite layers exhibit rhythmic repetition in this interval. The average rate of penetration was approximately 1.20m/hr. [31].

Between 2572m and 2628m (Adaiyah Formation), the lithology was mainly composed of anhydrite with thin beds of dolostone, observed by elevated (ρb) values, which were mostly greater than 2.9 g/cm³, PEF values exceeding 4 barns/electron, and a negative neutron porosity response. The average rate of penetration was approximately 1.34m/hr. [31].

Shale volume calculation

Gamma-ray logs, which quantify a formation's overall radioactivity, can be used to identify lithologies and correlate zones. They also aid in determining the amount of shale within reservoirs; the first step is to identify the index gamma ray using the equations proposed by Asquith and Gibson. [48].

$$GRI = \frac{GRlog - GR\ min}{GR\ max - GR\ min} \quad \dots (1)$$

Where:

GRI: Gamma Ray Index

GRlog: Gamma-ray reading from the log

GRmin: minimum gamma-ray response from the log. GRmax: maximum gamma-ray response from the log.

The Larinove's (1969) equation is used for older rocks, which we employed to calculate shale volume.$Vsh = 0.33 \times 2^{2\times GRI} - 1$ … (2)

The shale volume was calculated for the Alan, Mus, and Adaiyah formations in the MW-2 Well. The results indicate that shale content is significantly higher in the Alan Formation. Shale progressively decreases from the shale and shaly zones of the Alan and Mus formations to the clean zone of the Adaiyah Formation between 2480m and 2572m. The Mus Formation exhibited a high gamma-ray response, with a maximum value of approximately 109.2 API at a depth of 2546 m in MW-2, attributed to the high concentration of

radioactive minerals. In contrast, the Adaiyah Formation showed the lowest gamma-ray levels, reflecting its predominantly clean composition, primarily anhydrite. A minimum gamma ray value of 13.03 API was recorded at a depth of 2548.5m within the Mus Formation, corresponding to a minimal shale volume of less than 10%, as noted by (50). It was a clean zone (as illustrated in Fig. 8).

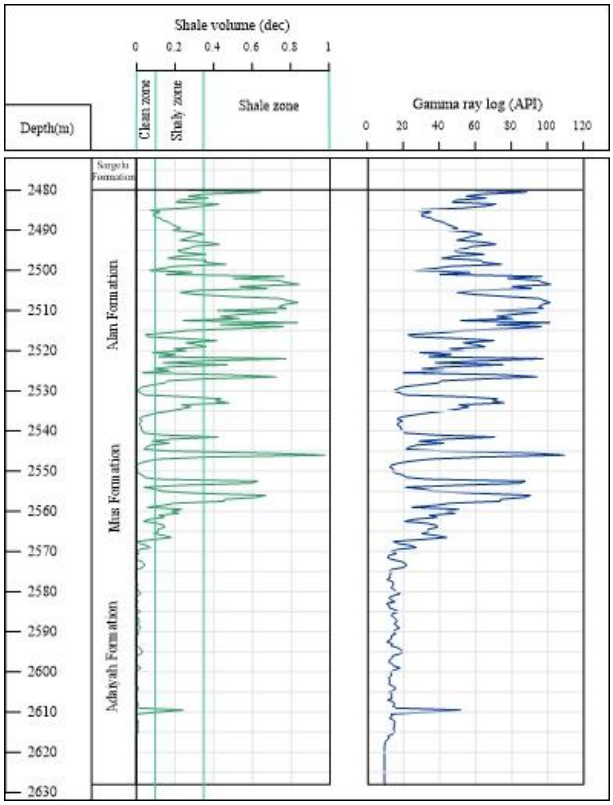

Fig. 8: Gamma ray log, shale volume calculation for Adaiyah, Mus, and Alan formations within MW-2 Well.

Porosity calculation

Porosity is a fundamental property of reservoir rocks, representing the void spaces within the rock volume that can store formation fluids, and is typically expressed as a percentage or fraction. (45). In petrophysical analysis, porosity is critical for evaluating reservoir capacity. Carbonate rocks exhibit more complex porosity systems than siliciclastic, including both primary porosity formed during deposition and secondary porosity resulting from diagenetic processes such as dissolution, tectonic deformation, and collapse. (51) Key porosity types include primary (inter-crystalline and inter-granular), secondary, effective (fluid-conductive), interconnected, and total porosity. (52). Total porosity encompasses all pore types, including fractures, vugs, joints, and channels. (53).

Porosity estimation from well logs using acoustic, density, and neutron tools requires accurate identification of both the matrix lithology and the drilling fluid composition. (45). The sonic log incorporates lithology and fluid-transit time, whereas density logs rely on matrix and fluid-density assessments. Neutron logs typically use water-saturated limestone as a calibration reference. (45, 47).

Porosity estimation from Sonic log

A sonic log is a measurement of the compressional sound wave velocity's interval transit time via formation along the borehole. It is represented as Δt or DT in microseconds/foot (μs/ft). The interval transit time depends upon both lithology and

porosity. Therefore, a formation matrix interval transit time must be known to derive sonic porosity. We used the Wyllie time-average equation in [48].

$$\Phi s = \frac{\Delta tlog - \Delta tmatrix}{\Delta tfluid - \Delta tmatrix} \quad \dots (3)$$

Where: Φs: Sonic porosity (decimal) Δt log: Log reading interval transit time in a formation (μs/ft) Δt matrix: Formation's matrix interval transit time (μs/ft) Δt fluid: Mud filtrate transit time (fresh water-based mud: 189 μs/ft, salt water-based mud: 185 μs/ft)

Sonic porosity calculations for the Alan, Mus, and Adaiyah formations in the studied wells utilized Δt matrix values of 45 μs/ft for dolomitic limestone, as recommended by [45]We utilized Δt matrix values of 43.5 μs/ft for dolostone and 50 μs/ft for anhydrite, given that all wells were drilled with fresh-based mud, a Δt fluid value of 189 μs/ft was applied.

Porosity estimation from the density log

The density log records the electron density of a formation, which correlates with its bulk density (ρb) in g/cm^3. The matrix density for porosity calculations was carefully selected based primarily on the lithology identified through the NΦ-Δt, NΦ-ρb, and PEF- ρb cross plots, matrix density values of 2.80 g/cm^3 for dolostone, as recommended by [45] 2.88 g/cm^3 and 2.98 g/cm3 were utilized for dolomitic limestone and anhydrite, and we also employed fresh mud at 1g/cm3 for all studied wells. The formula can be used to calculate the density porosity. [48].

$$\Phi D = \frac{\rho ma - \rho b}{\rho ma - \rho fl} \quad \dots (4)$$

Where: ΦD: Density porosity (decimal) ρma: Matrix density (g/cm^3)

ρb: Log reading bulk density (g/cm^3)

ρfl: Fluid density (1.0 g/cm^3) for freshwater-based mud, 1.1 g/ cm^{3}for saltwater-based mud.

Porosity estimation from neutron log

The neutron log quantifies the liquid-filled porosity; the porosity filled with water or oil and represents it as a percentage or porosity unit (ΦN, PHIN, or NPHI). Neutron logs are porosity logs measured directly that quantify the hydrogen index in the formation.

Correction for porosity from the shale effect

The presence, type, and distribution mode of clay minerals significantly impact reservoir storage. Consequently, porosity values were corrected for shale effects using appropriate equations for each porosity type. The following formulas were applied according to the proposed methodologies. [54]: for all types of porosity.

$$\Phi Se = \Phi S - Vsh \times \Phi Ssh \quad \dots (5)$$

where:

ΦSe = effective (shale-corrected) sonic porosity

ΦS = sonic porosity

ΦSsh = sonic porosity of a nearby shale

Vshale = shale volume.

$$\Phi De = \Phi D - Vsh \times \Phi Dsh \quad \dots (6)$$

where:

ΦDe =effective (shale-corrected) density porosity

ΦD = density porosity

ΦDsh = density porosity of a nearby shale

Vshale = shale volume.

$$\Phi Ne = \Phi N - Vsh \times \Phi Nsh \quad \dots (7)$$

where:

ΦNe = effective (shale-corrected) neutron porosity

ΦN = neutron porosity

ΦNsh = neutron porosity of a nearby shale

Vshale = shale volume.

Porosity logs in MW-2 reveal significant variability within the studied section. After correcting for shale content, porosity is significantly reduced. Notable variations in porosity were evident in the Alan and the upper part of the Mus formations (as presented in Fig.9). In contrast, the lower part of the Mus and the Adaiyah formations display relatively uniform and very low porosity values, due to the predominance of evaporite lithology.

Total porosity

In general, the proportion of a rock's pore space to its bulk volume can be used to estimate total porosity using Schlumberger's equation. [55].

$$\Phi T = \frac{\Phi Ne + \Phi De}{2} \quad \dots (8)$$

DOI: *https://doi.org/10.25130/tjps.v31i3.2003*

Where: ΦT: total porosity ΦNe: effective neutron porosity ΦDe: effective density porosity.

Fracture index

Fracture index or secondary porosity results from geological processes, such as diagenesis and catagenesis, that occur after sediment deposition. Vugs and fractures are not accounted for in the calculated sonic porosity, leading to an underestimation of porosity in carbonate rocks that contain them. Consequently, the secondary porosity (vugs or fractures) can be quantified from neutron and/or density porosity using the following equation proposed by Asquith and Gibson. [48].

$$\Phi F = \Phi T - \Phi Se \quad \dots (9)$$

Where: ΦF: fracture porosity (secondary porosity), ΦT: (total porosity), ΦSe: effective Sonic porosity (primary porosity). Overall, porosity values were predominantly negligible to poor, in line with the classification. [56]. The effective porosity values remain well below 0.1 (as shown in Fig. 9), indicating limited fluid storage capacity. The maximum porosity value was 0.14 at a depth of 2565m within the Mus Formation. The presence of secondary porosity within a restricted zone is observed from fracture index (ΦT-ΦS) shading and is also documented in the Heritage Oil Company. [31]. In addition to that, the interval between 2560m and 2567m displays an unusual trend with high-density porosity readings contrasted by considerably lower neutron porosity values (ΦD - ΦN crossover); this difference indicates a possible presence of gas in this interval. [57], likely associated with vugs or fractures. Supporting this interpretation, the gas chromatograph recorded a total gas content of approximately 9.5% during drilling measurement (MWD) [31]. Porosity measurements in the Adaiyah Formation between 2572m and 2628m are predominantly negligible, frequently recording zero or even negative values. This is attributed to the pervasive presence of anhydrite, which effectively reduces porosity within the formation. Generally, porosity values for the Adaiyah, Mus, and Alan formations indicate poor reservoir quality, acting mainly as seals rather than reservoirs (as shown in Fig. 9).

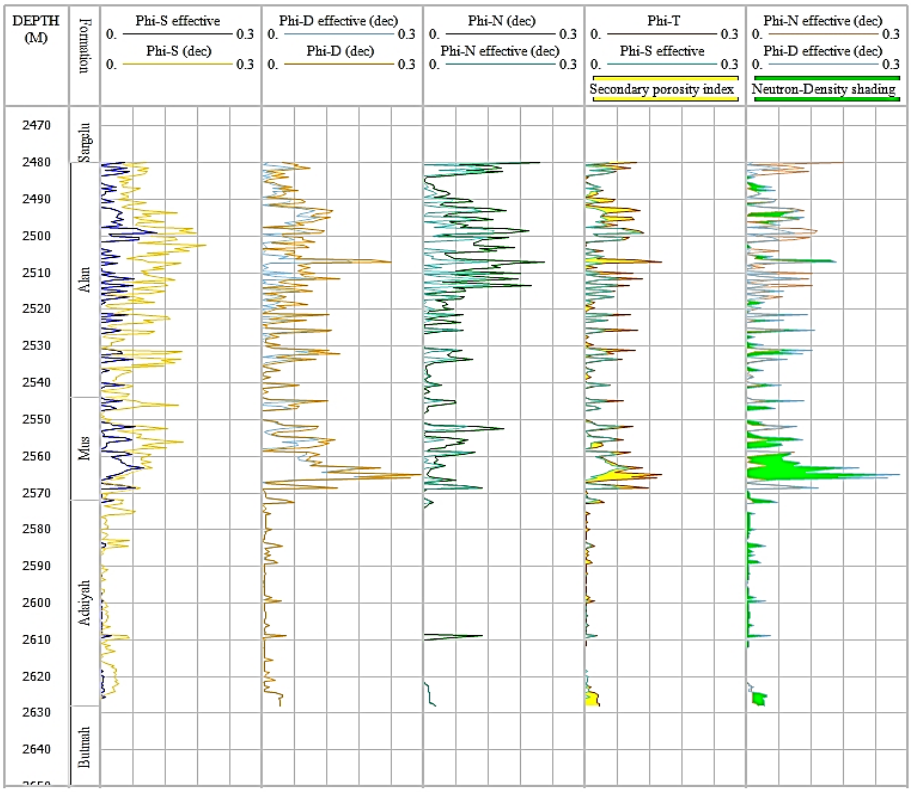

Fig.9: Curves plot of Sonic, Density, Neutron porosity before and after shale correction along with secondary porosity; moreover, Neutron-Density curves crossover for Alan, Mus, and Adaiyah formations between depth ranges 2480 and 2628 m in MW-2.

Permeability calculation

This study employed a multilinear regression (MLR) method to predict permeability (K) directly from associated well-log data (as represented in Fig.10). This predictive model utilizes well-log parameters, including gamma-ray (GR), bulk density (ρb), neutron porosity (ΦN), and compressional wave transit time (ΔT). The mathematical relationship is expressed as follows. [58].

$$Log\ k = -2.488 - 0.0073 * GR - 0.619 * \rho b + 11.128 * \Phi N + 0.050 \times \Delta t \quad \ldots (10)$$

Permeability values were predominantly poor to fair, as recommended by North. [56] predominantly below 0.1mD, which serves as a cut-off value, due to the high distribution of shale in the upper part and predominantly consists of Anhydrite and hard carbonate in the lower part, especially from an interval from 2572 m to 2628 m, indicating the rock matrix has limited capacity to allow fluid flow.

To minimize shale's influence on the evaluated parameters, we followed Taghavi's methodology. [58], modifying the adjustment factor from -2.488 to -3.88. This modification was implemented to more effectively eliminate the shale effect and better reflect the actual reduction in permeability under real conditions. By incorporating the new parameter into the calculation, the adjusted factor leads to a noticeable decrease in the measured permeability values.

K=10^(-3.88-0.0073*GR-0.619*ρb+11.128*ΦN+0.050*Δt)

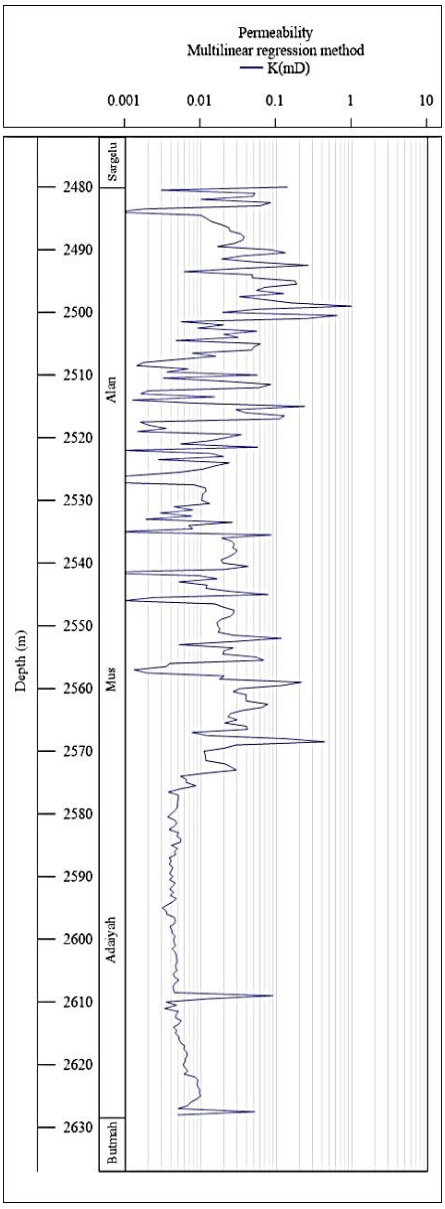

Fig. 10: Calculated permeability from MLR method for Adaiyah, Mus, and Alan formations between 2480-2628 m in well MW-2.

Cut-off and reservoir thickness determination

Cut-off calculation is a crucial method for defining the boundaries of effective reservoir zones. It helps identify the minimal petrophysical properties needed for a reservoir to be productive, including permeability, porosity, shale volume, and water saturation. The main aim of the cut-off calculation is to ensure accurate reserve estimation. To indicate the productive zone from the non-

productive zone, we used well log data to estimate cutoff values.

Shale Volume Cutoff

Shale cutoff is a critical parameter in reservoir characterization, referring to the maximum allowable shale content that maintains the reservoir's effectiveness. Excessive shale content in the reservoir acts as a barrier to fluid flow, significantly impacts reservoir permeability and reduces the transmission of hydrocarbon. This study utilized a shale volume of 0.35 as the cutoff value based on [50] for the Alan, Mus, and Adaiyah formations in MW-2 Well. A porosity-permeability cross-plot, with the primary objective of determining the porosity cut-off value. This crucial step involves utilizing the linear regression method, as described by [59], to derive the relationship between permeability and porosity.

The permeability cut-off values, defined as 1 mD for oil reservoirs and 0.1 mD for gas reservoirs, serve as benchmarks for determining the porosity cut-off. The porosity-permeability relationship is used to establish a linear regression model, and the porosity cut-off value of 0.07 is determined using the permeability cut-off criterion (as shown in Figs. 11 and 12).

Reservoir thickness determination

This study utilized lithology to determine the gross reservoir thickness, while shale volume cut-off, porosity, and permeability cut-off to estimate the net reservoir thickness.

However, the total thickness of the Alan, Mus, and Adaiyah formations in well MW-2 is approximately 148 m, with 26m consisting of shale and 67.5 m comprising anhydrite. The gross reservoir thickness in well MW-2 is approximately 54.5 m, primarily consisting of carbonate succession, while the net reservoir thickness, including some restricted zones, is estimated to be around 2.5 m (as illustrated in Fig.12). The limited net reservoir thickness suggests the very restricted part of the carbonate succession of Mus and Alan formations exhibits reservoir potential primarily due to diagenetic modification and facies variability, in addition, Adaiyah formation mainly consists of anhydrite from 56 total thickness of the Formation, 53.5m including evaporate.

DOI: *https://doi.org/10.25130/tjps.v31i3.2003*

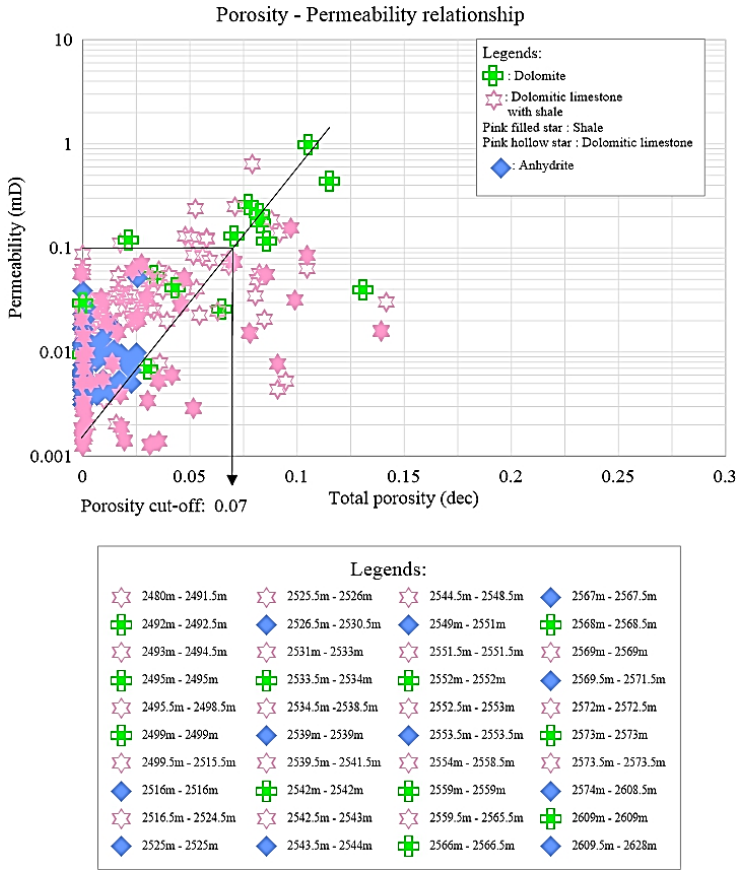

Fig. 11: Porosity and permeability relationship for Adaiyah, Mus, and Alan formations at depth 2480-2628 m to estimate porosity cut-off values from permeability cut-off values associated with gas reservoirs for well MW-2.

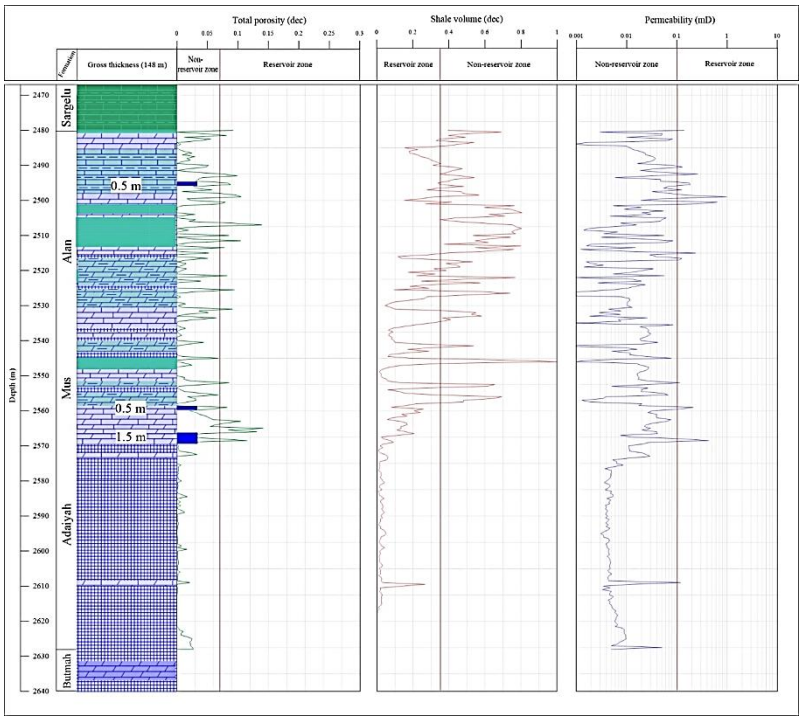

Fig. 12 shows the determination of net reservoir thickness from porosity, shale volume, and permeability cutoff values between depths 2480m and 2628 m for Adaiyah, Mus, and Alan formations within MW-2 Well.

CONCLUSION

1. Stratigraphic and Lithological Observations:
Although the total drilled thickness of the Alan, Mus, and Adaiyah formations in ell MW-2 is approximately 148 m (64 m for Alan, 28 m for Mus, and 56 m for Adaiyah, based on the geological report), no distinct log-stratigraphic boundaries were observed between these formations. Instead, a continuous vertical facies transition is evident, beginning with interbedded carbonate rocks, shale, and argillaceous limestone at the top, followed by the appearance of evaporite layers at ~2516 m. The frequency and thickness of these evaporites increase progressively with depth, fully dominating the interval from 2572 to 2628 m, where they are interbedded with anhydrite layers.

2. Porosity Characteristics:
Porosity is predominantly negligible to poor, with effective porosity values generally below 0.1, indicating limited fluid storage capacity. Secondary porosity is minimal and highly lithology-dependent, occurring in only very restricted intervals. A maximum porosity of 0.14 was observed at a depth of 2565 m within the Mus Formation. The interval from 2560 m to 2567 m exhibits a ΦD–ΦN crossover, indicative of gas in fractures or vugs, a conclusion supported by gas chromatograph data.

3. Permeability Evaluation:
Permeability is generally poor to fair, with most values falling below 0.1 mD, supporting the use of this threshold as a permeability cut-off. The poor reservoir quality is attributed to the high shale content in the upper section and the dominance of anhydrite and dense carbonate rocks in the lower section. Some improved permeability is observed in intervals such as 2572–2628 m, though still limited in extent.

4. Reservoir Thickness Estimation:
Porosity cut-off values were identified as 0.07% from gas permeability (0.1 mD), with a shale cut-off value (0.35%) used to distinguish net reservoir thickness. Of the total 148 m drilled interval of Adaiyah, Mus, and Alan formations, 26 m comprises shale, and 67.5 m consists of anhydrite. The gross reservoir thickness is estimated at approximately 54.5 m, mainly made up of carbonate sequences, while the net reservoir thickness is limited to about 2.5 m, along a few narrow zones.

5. Overall Assessment:
Based on lithological, porosity, shale contents, and permeability analyses, the studied section lacks significant reservoir characteristics. However, due to its thick anhydrite, shale, and compact carbonate composition, it may function effectively as a local cap rock for a potential underlying Butmah reservoir.

Conflict of interest: The authors declared no conflicts of interest.

Sources of funding: This research did not receive any specific grant from funding agencies in the public, commercial, or not-for-profit sectors.

Author contributions: The authors contributed equally to the study.

REFERENCES

1. Murris RJ. Middle East: Stratigraphic Evolution and Oil Habitat. In: Demaison G, Murris RJ, editors. Petroleum Geochemistry and Basin Evaluation. 35: American Association of Petroleum Geologists; 1984. p. 0. https://doi.org/10.1306/2f918a8b-16ce-11d7-8645000102c1865d

2. Beydoun ZR. Arabian plate hydrocarbon geology and potential—a plate tectonic approach: American Association of Petroleum Geologists; 1991. https://doi.org/10.1306/St33533

3. Sadooni FN. Stratigraphic sequences and petroleum habitat of the Jurassic system in the Arabian Gulf Basin. GeoArabia. 1995;1(3):467–89.

4. Simmons MD, Davies RB, Hall SH, Heward AP, Horbury AD. Arabian plate sequence stratigraphy. Journal name not specified. 2001.

5. Aqrawi AA, Goff JC, Horbury AD, Sadooni FN. The petroleum geology of Iraq: Scientific Press, Beaconsfield, UK; 2010.

6. Abdula RA. Organic geochemical assessment of Jurassic potential source rock from Zab-1 well, Iraqi Kurdistan. Iraqi Bulletin of Geology and Mining. 2016;12(3):53-64.
7. Abdula RA, Ali MA, Ahamad MM, Hamad HR. Rock-Eval Pyrolysis Results from the Bijeel 1 Well, Kurdistan Region, Iraq. ZANCO Journal of Pure and Applied Sciences. 2017;29(3):33-42.
8. Rashid F. Reservoir productivity analysis of intercalated limestone and anhydrite beds in Zagros Folded Belt, Kurdistan Region of Iraq. Kurdistan Journal of Applied Research. 2020;5(1):1-15. https://doi.org/https://doi.org/10.24017/science.2020.1.1
9. Al-Atroshi SJ, Sherwani GH, Al-Naqshbandi SF. Hydrocarbon Potential of the Middle–Late Jurassic Series of Northwestern Iraq: A Case Study in the Shaikhan Oil Field. UKH Journal of Science and Engineering. 2020;4(2):48-64. https://doi.org/https://doi.org/10.25079/ukhjse.v4n2y2020.pp48-64
10.Edilbi ANF. Comparative Study on Hydrocarbon Generation in Different Tectonic Zones: A Case Study from the Upper Jurassic Naokelekan Formation at the Imbricated and High Folded Zones, Kurdistan Region, Iraq. UKH Journal of Science and Engineering. 2020;4(2):24-34.
11.Baban DH, Ahmed SM. Source rocks' potentiality of the Sargelu Formation (Middle Jurassic) in the Taq Taq Oilfield, Kurdistan Region, Iraq. The Iraqi Geological Journal. 2021:59-85. https://doi.org/10.46717/igj.54.2E.5Ms-2021-11-21
12.Albeyati FM, Abdula RA, Othman RS. Organic geochemistry of the Middle to Upper Jurassic source rocks succession in Balad-1 Well, Balad Oil Field, Central Iraq. 2021.
13.Mahdi AQ, Abdel-Fattah MI, Hamdan HA. An integrated geochemical analysis, basin modeling, and palynofacies analysis for characterizing mixed organic-rich carbonate and shale rocks in the Mesopotamian Basin, Iraq: Insights for multisource rocks evaluation. Journal of Petroleum Science and Engineering. 2022;216:110832. https://doi.org/10.1016/j.petrol.2022.110832
14.Dohan AH, Hassan FN, Kadhim LS. Depositional Environment of Middle Jurassic Sargelu Formation Based on Petrographical Study in Selected Wells at Balad, Ajil, and Baiji Oilfields, Central Iraq. Tikrit Journal of Pure Science. 2022;27(3):31-42. https://doi.org/10.25130/tjps.v27i3.53
15.Mohammed-Sajed OK, Glover PW. Influence of anhydritisation on the reservoir quality of the Butmah Formation in north-western Iraq .Marine and Petroleum Geology. 2022;135:105391. https://doi.org/10.1016/j.marpetgeo.2021.105391
16.Al-Shammary M, Malak ZA, Al-Jwary M. Sedimentological Study of Exposed Successions of the Sargelu Formation, Middle Jurassic, Northeastern, Iraq. The Iraqi Geological Journal. 2023:51-63. https://doi.org/10.46717/igj.56.1B.5ms-2023-2-13
17.Qin G, Wang Y, editors. Jurassic Hydrocarbon System Appraisal and Implications for Prospectivity in Central and Southern Iraq, Middle East. Abu Dhabi International Petroleum Exhibition and Conference, 2023: SPE.
18.Al-Tarim HA. Microfacies Analysis and Diagenetic Effects of Middle Jurassic Succession in Rania and Sargelu Sections, Northern Iraq. The Iraqi Geological Journal. 2023:68-83. https://doi.org/doi:10.46717/igj.56.1E.6ms-2023-5-16
19.Ahmed A, Al-Hameedy R. Sedimentological Study of the Chia Gara Formation Successions in Selected Outcrop Sections of Northern Iraq. Iraqi National Journal of Earth Science. 2023;23(2):1.0-18.0. https://doi.org/10.33899/earth.2022.134929.1020
20.Mina CT, Abdula RA. Hydrocarbon potential, source correlation, and paleoenvironmental reconstruction of the Jurassic interval in the Zey Gawra Oilfield, Kurdistan Region, Iraq. Bulletin of the Geological Society of Malaysia. 2024;78. https://doi.org/10.7186/bgsm78202409

21.Khalaf A, Alkhafaji MW. Organic matter characteristics and hydrocarbon potential of Jurassic Sargelu Formation in X Well, Northern Iraq. The Iraqi Geological Journal. 2024:52–64. https://doi.org/10.46717/igj.57.2D.4ms-2024-10-14

22.Rasool RH, Ali SA, Al-Juboury AI, Rowe H, Zanoni G. Mineralogical Implications of the Middle to Upper Jurassic Succession at Sargelu Village in Sulaymaniyah City, Northeastern Iraq. Iraqi National Journal of Earth Sciences. 2024;24.(2). https://doi.org/10.33899/earth.2023.143790.1155

23.Muhammad SA, Saeed AT. Dolomitization of the Lower Part of the Sargelu Formation, Northeastern Iraq. Tikrit Journal of Pure Science. 2024;29(1):136-48. https://doi.org/10.25130/tjps.v29i1.1484

24.Omar N. Sedimentology and geochemistry of the Jurassic system in northern Iraq: Implications for paleoenvironmental reconstruction, provenance and tectonic setting: Universitäts-und Landesbibliothek Bonn; 2024.

25.Jassim S, Buday T, Cicha I, Prouza V. Late Permian-Liassic megasequence AP6. Geology of Iraq, Dolin, Prague and Moravian Museum, Brno, Czech Republic. 2006:104-16.

26.Al-Husseini MI. Jurassic sequence stratigraphy of the western and southern Arabian Gulf. GeoArabia. 1997;2(4):361-82. https://doi.org/10.2113/geoarabia0204361

27.English JM, Lunn GA, Ferreira L, Yacu G. Geologic evolution of the Iraqi Zagros, and its influence on the distribution of hydrocarbons in the Kurdistan region. AAPG Bulletin. 2015;99(2):231-72. https://doi.org/10.1306/06271413205

28.Al-Badran MA, Al-Jubouri AM. Tectonostratigraphic evolution and petroleum systems of the Lower Jurassic in Iraq. Journal of Petroleum Geology. 2017;40(2):129–146.

29.Al-Bassam RS, Al-Mansoori WS, Al-Saad DH. Petrophysical properties of the Lower Jurassic carbonates and their impact on hydrocarbon accumulation in Iraq. Journal of Petroleum Science and Engineering. 2019;174:1005–1020.

30.Oil H. Miran Field Evaluation Report. 2011.

31.Oil H. Master Log: Miran-2 (MW-2). Kurdistan, Iraq; 2009.

32.SHS A-H. Geometric analysis and structural evolution of the NW Sulaimani area, Kurdistan Region, Iraq. Thesis (PhD): University of Sulaimani, 2011.

33.Zangana HA, Sherwani GH, Tawfeeq YJ, Al-Ansari N. Reservoir characterization of the Early Jurassic Butmah Formation using well log data in selected wells from Iraqi Kurdistan Region. Open Journal of Geology. 2020;10(12):1173-88. https://doi.org/10.4236/ojg.2020.1012057

34.Altaee NT, Malak ZA. Facies Analysis and Depositional Environments of the Ubaid Formation, Western Iraq. Iraqi Journal of Science. 2021:2580-8. https://doi.org/10.24996/ijs.2021.62.8.11

35.Ali RA, Jassim HK. The mineralogy, geochemistry and the origin of the lower clastic unit in Hussainiyat Formation–Western Desert of Iraq: The origin of the lower clastic unit in Hussainiyat Formation. Iraqi Bulletin of Geology and Mining. 2022;18(1):1–19.

36.Ali MS, Al-Dabagh MM, Asaad IS, editors. Determination of porosity types in the Butmah Formation (early Jurassic) in selected wells, Northern Iraq (case study). AIP Conference Proceedings; 2022: AIP Publishing.

37.Delizy BA, Shingaly WS. Microfacies Analysis and Depositional Environment of Sarki Formation (Early Jurassic), Rawanduz Area, Kurdistan Region, Northern Iraq. Tikrit Journal of Pure Science. 2022;27(1):24-35. https://doi.org/10.25130/tjps.v27i1.79

38.Omar N, McCann T, Al-Juboury AI, Ustinova MA, Sharezwri AO .Early Jurassic–Early Cretaceous Calcareous Nannofossil Biostratigraphy and Geochemistry, Northeastern Iraqi Kurdistan: Implications for Paleoclimate and Paleoecological Conditions. Geosciences. 2022;12(2):94. https://doi.org/10.3390/geosciences12020094

39. Omar N, McCann T, Al-Juboury AI, Franz SO, Zanoni G, Rowe H. A comparative study of the paleoclimate, paleosalinity and paleoredox conditions of Lower Jurassic-Lower Cretaceous sediments in northeastern Iraq. Marine and Petroleum Geology. 2023;156:106430. https://doi.org/http://dx.doi.org/10.1016/j.marpetgeo.2023.106430

40. Al-Jaleel HS, Tobia FH, Ahmed IN, Al-Jaleel BH. Geochemical characteristics of dolomite: a case study from lower Jurassic formations, imbricated zone, Iraqi Kurdistan region. Carbonates and Evaporites. 2024;39(4):99. https://doi.org/http://dx.doi.org/10.1007/s13146-024-01012-w

41.Bellen RC, Dunnington HV, Wetzel R, Morton D. Lexique Stratigraphique International Asie, Iraq. 1959. 333 p.

42.Oil H. Master Log: Miran-3 (MW-3). Kurdistan, Iraq; 2012.

43.Oil H. Master Log: Miran-4 (ME-1). Kurdistan, Iraq: DQE International; 2012.

44.Buday T. The regional geology of Iraq: stratigraphy and paleogeography: State Organization for Minerals, Directorate General for Geological Survey …; 1980.

45.Asquith GB, Krygowski D, Gibson CR. Basic well log analysis: American Association of Petroleum Geologists, Tulsa, 2004.

46.Tiab D, Donaldson EC. Petrophysics: theory and practice of measuring reservoir rock and fluid transport properties: Elsevier; 2024.

47.Schlumberger. Log interpretation principles/applications. The editor. Sugar Land, TX: Schlumberger Well Services Inc.; 1989.

48.Asquith GB, Gibson CR. Basic relationships of well log interpretation: Chapter I. 1982.

49.Radwan AE. New Petrophysical Approach and Study of the Pore Pressure and Formation Damage in Badri, Morgan and Sidki Fields, Gulf Of Suez Region, Egypt 2018.

50.Nouh AZ. The relation between the shale origin (source or non-source) and its type for Abu Roash formation at Wadi El-Natrun area, south of Western Desert, Egypt. Australian Journal for Basic and Applied Sciences. 2008;2(3):360.

51.Dasgupta R, Mukherjee S. Fundamentals of Structural Geology. Cham: Springer; 2020.

52.Heinemann Z, Mittermeir G. Fluid flow in porous media. 2013.

53.Schlumberger. Log interpretation charts. Houston: Schlumberger Wireline & Testing; 1997.

54.Dewan J. Essentials of modern open-hole log interpretation. 1983.

55.Schlumberger. Log interpretation principles and applications. New York: Schlumberger; 1987.

56.Petroleum geology. nd, editor. London: Allen & Unwin; 1985.

57.Qader FM, Ali SM. Reservoir Characteristics of the Lower Miocene Carbonate Formations in Kor Mor Gasfield, Kirkuk Area, NE Iraq. Tikrit Journal of Pure Science. 2022;27(3):43-52. https://doi.org/10.25130/tjps.v27i3.52

58.Taghavi M. Application of multilinear regression to predict permeability from well log data. Journal of Petroleum Science and Engineering. 2005;48(3–4):243–257.

59.Sampson RJ. Statistics and data analysis in geology. New York: Wiley; 1986.